

# 3D Orientation Estimation With Configurable Backscatter Arrays

Mohamad Rida Rammal\*, Suhas Diggavi\*, and Ashutosh Sabharwal†

\*Department of Electrical and Computer Engineering, UCLA.

†Department of Electrical and Computer Engineering, Rice University.

**Abstract**—We consider the problem of estimating the orientation of a 3D object with the assistance of configurable backscatter tags. We explore the idea of designing tag response codes to improve the accuracy of orientation estimation. To minimize the difference between the true and estimated orientation, we propose two code design criteria. We also derive a lower bound on the worst-case error using Le Cam’s method and provide simulation results for multiple scenarios including perfect and imperfect channel knowledge, comparing the performance of various coding methods against the suggested designs.

## I. INTRODUCTION

3D orientation tracking is an important function in many domains, e.g., in robotics, aerospace, and medicine. Orientation can be estimated using many methods, e.g., inertial sensors can be mounted on the object whose orientation has to be measured. Orientation can also be measured using a computer vision based methods [1]–[4]. Each of the existing methods have their own pros and cons. For example, inertial sensors may not be suitable for many Internet-of-Things applications, e.g., tracking packages where the solutions have to be very cost-effective. Additionally, the performance of computer vision methods depends on light conditions, and can be confused for objects that exhibit symmetries. As an extreme example of that last problem, one can rotate a cube in many ways such that it would look precisely the same as it did prior to rotation.

Wireless sensing has emerged as an interesting alternative sensing modality. Radio-frequency based methods can be useful when visible light wavelengths are not effective, e.g., cases with poor visibility or non-line-of-sight scenarios. In particular, backscatter arrays have been recently used for geo-location and 3D orientation estimation [5]–[8]. Using backscatter arrays is philosophically akin to “painting the faces” of an object, making it a promising option for the orientation detection of symmetric objects such as the solid cube in the last example. In this work, we study 3D orientation estimation with the help of configurable backscatter arrays.

In order to aid with the estimation task, one can design the backscatter response to received signals. Specifically, we design the backscatter responses by changing their reflection coefficients. The design can be captured as a binary code specifying what or when the backscatter tags reflect. The problem of finding the best code for the estimation task was first formulated and explored in [9], where we proposed a heuristic

This work is supported in part by NSF grants 1955632, 2146838, 1956297.

code design criterion and had a preliminary exploration of the systems performance.

**Contributions:** In this paper, we revisit the problem and expand our understanding in the following ways. First, we propose two analytic code design criteria that depend on channel knowledge, and investigate their performance with respect to a baseline orthogonal code. We also develop a lower bound on the worst-case error, which quantifies the systems performance with respect to channel parameters such as the number of antennas and the number of tags used. Finally, we provide a comprehensive numerical exploration of the systems performance, including the robustness of the design criteria against imperfect channel knowledge.

By numerically evaluating the performance, we observe the following. Our design criteria yield codes that offer significant advantages over the channel-oblivious orthogonal code for both the average and worst-case error performance (see Section II-D for precise definitions). In some cases, our designs provide two orders of magnitude improvements in error performance. We also found that *precise* channel knowledge at the transmitter is not critical; Our design criteria are robust against channel estimation errors, retaining almost all improvements when computed with SNR values greater than or equal to 10dB.

**Related work:** In [9], we suggested a heuristic design criteria aimed at maximizing the average-case performance, but did not make attempts to assess its performance. Furthermore, we only considered the average-case error of the system, and did not study the worst-case error, explored in this paper. In [7], [8], [10], the authors present various methods for orientation estimation (2D or 3D) using backscatter tags, but do not explore the design of backscatter responses and its effect on the estimation problem. In [11], the authors use orthogonal codes (see Section IV for a definition) to distinguish the tags from each other and the environment. However, none of these past works has considered optimal code design for 3D orientation sensing.

**Organization:** Section II describes the channel model and formulates the estimation problem. Section III describes the main results. Section IV provides various numerical results. Finally, the proofs of the theorems and lemmas shown in Section III can be found in Section V of the full-version of the paper [12]. Moreover, [12] contains additional numerical results among which is the performance of the design criteria

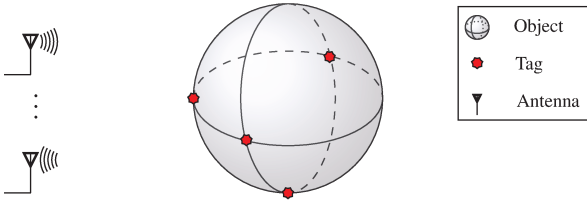


Fig. 1: The components of the considered system. The object along with the tags, rotate around a specific point (in this case, the center of the sphere). The full-duplex antennas interrogate the configurable tags and receive back the reflected signal. We then use the received signal to infer the orientation.

on random tag arrays and the effect of multipath.

## II. PROBLEM FORMULATION

### A. Notation

$\mathbb{R}^k$  and  $\mathbb{C}^k$  are the sets of real-valued and complex-valued  $k$ -dimensional vectors, respectively.  $A^T$  and  $A^H$  denote the transpose and conjugate transpose of the matrix  $A$ . If  $\mathbf{x}$  is a vector with  $n$  elements, then  $\text{diag}(\mathbf{x})$  denotes the  $n \times n$  square matrix with the elements of  $\mathbf{x}$  on its main diagonal;  $\|\cdot\|$  is the standard Euclidean norm on vectors, and  $\|\cdot\|_F$  is the Frobenius norm on matrices.

### B. System Model

We assume a system having  $K$  full-duplex antennas with position vectors  $\mathbf{x}_1^{\text{ant}}, \dots, \mathbf{x}_K^{\text{ant}} \in \mathbb{R}^3$ , and  $N$  backscatter tags with position vectors  $\mathbf{x}_1^{\text{tag}}, \dots, \mathbf{x}_N^{\text{tag}} \in \mathbb{R}^3$ . We consider an object on which we place the  $N$  configurable backscatter tags. The object can freely rotate around a specific point in space. For ease of computation, we consider the coordinate system in which the point that the object rotates around is the center  $\mathbf{0} = [0, 0, 0]^T$  (see Figure 1).

We specify the orientation of the object using a rotation matrix  $Q \in SO(3) \subseteq \mathbb{R}^{3 \times 3}$ , where  $SO(3)$  is the 3D rotation group. If the object has tags with positions  $\mathbf{x}_1^{\text{tag}}, \dots, \mathbf{x}_N^{\text{tag}}$  on it, and a rotation  $Q$  is applied to the object, the tags would have the new positions  $Q\mathbf{x}_1^{\text{tag}}, \dots, Q\mathbf{x}_N^{\text{tag}}$  (see Figure 2). In this framework, we specify the original orientation of the object using the  $3 \times 3$  identity matrix  $I_3$ .

Each backscatter tag can be configured by setting its state to a value  $i \in \{0, 1\}$ . The state, in turn, determines the reflectivity of the tag. For instance, we may choose to correspond a state of 0 to a reflectivity of  $+0.5$  and a state of 1 to a reflectivity of  $-0.5$ . In this scenario, tags reflect regardless of the their state. On the other hand, we may choose to correspond a state of 0 to a reflectivity of 0 (does not reflect), and a state of 1 to a reflectivity of 1 (reflects) i.e. the state determines the on-off condition of the tag. In addition, the state of each tag can either remain constant (passive) or change over time (active). We study the performance of both options.

The orientation of the object determines the position of the tags, and the states of the tags set their reflectivities. Hence,

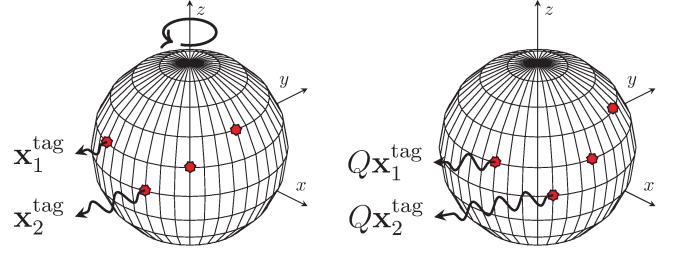


Fig. 2: Rotation of the object about the  $z$ -axis. When the object rotates, the tags rotate along with it. The new positions of the tags produce a different received signal. While the tags are equidistant from the point of rotation in the figure, this does not have to be the case.

the orientation and tag states determines the channel model, and in turn the received signal. We use the received signal to estimate the orientation of the object. Our goal is to analyze the performance of this system, and find the best set of tag states for the estimation task. We describe our channel model next. We use the following free-space path loss formula for line-of-sight propagation [13] between points  $\mathbf{x}_1, \mathbf{x}_2 \in \mathbb{R}^3$ :

$$\eta(\mathbf{x}_1, \mathbf{x}_2) = \frac{1}{4\pi \|\mathbf{x}_1 - \mathbf{x}_2\|} \exp\left(\frac{-2\pi j \|\mathbf{x}_1 - \mathbf{x}_2\|}{\lambda}\right), \quad (1)$$

where  $\lambda$  is the wavelength. In other words, suppose  $\mathbf{x}_{T_x}$  and  $\mathbf{x}_{R_x}$  are the position vectors of an isolated transmitter and receiver, and  $s_{T_x}$  and  $s_{R_x}$  the transmitted and received signals, respectively, then

$$s_{R_x} = s_{T_x} \eta(\mathbf{x}_{T_x}, \mathbf{x}_{R_x}). \quad (2)$$

We now specify the matrices involved in our channel model. Let  $H_Q$  be the  $K \times N$  matrix of the line-of-sight responses between the tags and antennas when the object is in orientation  $Q$ , i.e.  $(H_Q)_{k,n} = \eta(\mathbf{x}_k^{\text{ant}}, Q\mathbf{x}_n^{\text{tag}})$ . Let  $A$  be the symmetric  $K \times K$  matrix of inter-antenna line-of-sight responses with  $A_{k,k'} = \eta(\mathbf{x}_k^{\text{ant}}, \mathbf{x}_{k'}^{\text{ant}})$ . Let  $B$  be the symmetric  $N \times N$  matrix of the inter-tag channel responses when the object is in orientation  $Q$ . In other words,

$$(B_Q)_{n,n'} = \eta(Q\mathbf{x}_n^{\text{tag}}, Q\mathbf{x}_{n'}^{\text{tag}}) = \eta(\mathbf{x}_n^{\text{tag}}, \mathbf{x}_{n'}^{\text{tag}}). \quad (3)$$

Applying the same rotation to any two tags does not change the distance between them, so we can drop  $Q$  from the subscript of  $B_Q$  and use  $B$  instead. Now, let  $\mathbf{s}_t$  and  $\mathbf{s}'_t$  be the vectors of the transmitted signals at the antennas and tags respectively at time  $t$ , and  $\Psi_t$  and  $\Psi'_t$  be the vectors of the received signals at the antennas and tags respectively at time  $t$ . The relationship between these vectors is given by:

$$\begin{bmatrix} \Psi_t \\ \Psi'_t \end{bmatrix} = \begin{bmatrix} A & H_Q \\ H_Q^T & B \end{bmatrix} \begin{bmatrix} \mathbf{s}_t \\ \mathbf{s}'_t \end{bmatrix}. \quad (4)$$

As mentioned before, each backscatter tag can be configured by setting its state to a value  $i \in \{0, 1\}$ , which in turn determines its reflectivity  $r_i \in \mathbb{C}$ . Hence, the reflectivities can be expressed in terms of the states assigned to the tags. Letting  $s_{t,n}$  be the state of the  $n^{\text{th}}$  tag at time  $t$ ,  $\mathbf{c}_t = (s_{t,1}, \dots, s_{t,N})$

be the *codeword* at time  $t$  (a codeword is a vector of states), and  $r(\cdot)$  be the mapping from codewords to reflectivity vectors, we define the matrix of reflectivities at time  $t$  as:

$$R_t = \text{diag}(r(\mathbf{c}_t)). \quad (5)$$

Using the fact that the tags reflect the incident signals, the transmitted signal at the tags is given by  $\mathbf{s}'_t = R_t \Psi'_t$ . Substituting the value of  $\mathbf{s}'_t$  in (4), we obtain the following equations:

$$\Psi_t = A \mathbf{s}_t + H_Q R_t \Psi'_t \quad (6)$$

$$\Psi'_t = H_Q^T \mathbf{s}_t + B R_t \Psi'_t \quad (7)$$

Solving the above equations, we obtain that the received signal is given by  $\Psi_t = A \mathbf{s}_t + H_Q R_t (I - B R_t)^{-1} H_Q^T \mathbf{s}_t$ . Since the first term in the previous expression does not depend on  $Q$ , we can subtract it at the receiver<sup>1</sup> yielding a modified noiseless signal  $\mathbf{f}(Q; \mathbf{c}_t) \in \mathbb{C}^K$  given by:

$$\mathbf{f}(Q; \mathbf{c}_t) = H_Q R_t (I - B R_t)^{-1} H_Q^T \mathbf{s}_t. \quad (8)$$

### C. Codes

The expression in (8) is the *noiseless* channel output when using a codeword  $\mathbf{c}_t$ . Based on numerical simulations, we have observed that a single codeword often only allows us to detect some orientations, and not others. Specifically, all tag arrays we came across had the following property: for every codeword  $\mathbf{c} \in \{0, 1\}^N$ , there exists some  $Q, Q'$  such that  $Q \neq Q'$  and  $\mathbf{f}(Q; \mathbf{c}) \approx \mathbf{f}(Q'; \mathbf{c})$  (see Figure 7 in Section IV for such an array). In other words, for every codeword, there is a pair of orientations that the codeword makes almost indistinguishable based on the received signal.

Therefore, using different codewords over time is a natural extension to the model as a new codeword could fill in the gaps left by the ones used previously. Based on this intuition, we define a *code*  $C = [\mathbf{c}_1 \cdots \mathbf{c}_T] \in \{0, 1\}^{N \times T}$  to be a binary matrix where each column corresponds to the codeword at a specific time  $t$  (See Figures 3,4). Given the code  $C$ , we denote the *concatenated* channel output as (using  $F$  instead of  $f$ ):

$$F(Q; C) = [\mathbf{f}(Q; \mathbf{c}_1) \cdots \mathbf{f}(Q; \mathbf{c}_T)] \in \mathbb{C}^{K \times T}. \quad (9)$$

### D. Performance Measures

We consider estimation over a finite uniform subset of orientations  $\mathcal{Q} \subset \text{SO}(3)$ , and use the loss function  $\theta(Q, Q')$ , equal to the Frobenius norm between the two rotation matrices i.e.,

$$\theta(Q, Q') = \|Q - Q'\|_F. \quad (10)$$

Letting  $C$  be any code, and  $W$  be complex Gaussian noise, we define the noisy received signal as  $Y = F(Q; C) + W$ . Hence, the *unnormalized* average error of code  $C$  is given by:

$$\mathcal{L}(C) = \sum_{Q \in \mathcal{Q}} \mathbb{E}_W [\theta(\hat{Q}(Y), Q)], \quad (11)$$

where  $\hat{Q}(Y)$  is the minimum distance decoder to the grid of orientations  $\mathcal{Q}$  i.e., the MMSE estimator of  $Q$  given  $Y$ . Note if

<sup>1</sup>We are eliminating full-duplex self-interference, e.g., see [14].

Time \ Tag	1	2	...	T
1	■	■	...	■
2	■	■	...	■
⋮	⋮	⋮	⋮	⋮
N	■	■	...	■

Fig. 3: An illustration of coding over time. Different colors denote different states (reflectivities) of the tag, and different patterns of the states denote different codewords.

				Tag 1 States
				Tag N States
				$\mathbf{c}_T$
1	1	...	0	
0	0	...	1	
⋮	⋮	⋮	⋮	⋮
1	0	...	0	
				$\mathbf{c}_1 \mathbf{c}_2 \cdots \mathbf{c}_T$

Fig. 4: The associated matrix to the coding over time example in Figure 3

the orientation is considered a random variable, we implicitly assume a uniform prior over the orientations in  $\mathcal{Q}$ . Now, a code that minimizes the average error could still provide poor performance for a *particular* orientation. For this reason, we study the worst-case error as it delivers guarantees on the performance across all possible orientations. We define worst-case error (over all possible orientations in  $\mathcal{Q}$ ) as:

$$\mathcal{M}(C) = \max_{Q \in \mathcal{Q}} \mathbb{E}_W [\theta(\hat{Q}(Y), Q)]. \quad (12)$$

We suggest criteria for minimizing either depending on the application's particular requirements.

## III. MAIN RESULTS

Our goal is to find the best code for the estimation task. However,  $\mathcal{L}(C)$  in (11) and  $\mathcal{M}(C)$  in (12) are intractable. One route we could take is to investigate *tractable* upper or lower bounds on the errors, and minimize those bounds as a proxy for minimizing the errors themselves.

### A. Design Criterion For The Average Error

We obtain the upper bound on the average error by replacing the probability of misestimating the actual orientation of the object by a tractable quantity. The proof of the following result is given in Section V-A of [12].

#### Theorem III.1

Assuming complex white Gaussian noise, the average error  $\mathcal{L}(C)$  given in (11) is upper bounded by:

$$\mathcal{U}(C) = \sum_{Q, Q' \in \mathcal{Q}} \text{erfc} \left( \frac{\|F(Q; C) - F(Q'; C)\|_F}{2\sqrt{2}\sigma} \right) \theta(Q, Q'). \quad (13)$$

where  $\theta(Q, Q')$  is given in (10),  $\text{erfc}$  is the complement of the Gaussian error function, and  $\sigma$  is the standard deviation of the noise.

Hence, the design criteria for minimizing the average error is simply given by the optimization problem  $\min_C \mathcal{U}(C)$ . We can infer the following intuition from  $\mathcal{U}(C)$  in (13): good codes should map orientations that are far apart (in terms of  $\theta$ ) to channel outputs that are also far apart. Moreover, since  $\text{erfc}(x)$  is tightly upper bounded by  $\exp(-x^2)$ ,  $\mathcal{U}(C)$  implies that the distance between channel outputs  $\|F(Q; C) - F(Q'; C)\|_F$  has an inverse exponential relationship with the average error.

### B. Codes And Bounds For the Worst-Case Error

Whereas we optimize an upper bound for the average error in Section III-A, we obtain a lower bound on the worst-case error  $\mathcal{M}(C)$  using Le Cam's method [15], and minimize the bound to obtain a code for the worst-case performance. The proof of the following result is given in Section V-B of [12].

### Theorem III.2

Assuming complex white Gaussian noise, the worst-case error  $\mathcal{M}(C)$  given in (12) is lower bounded by:

$$\mathcal{V}(C) = \max_{Q, Q' \in \mathcal{Q}} \exp \left( -\frac{\|F(Q; C) - F(Q'; C)\|_F^2}{2\sigma^2} \right) \frac{\theta(Q, Q')}{4}, \quad (14)$$

where  $\theta(Q, Q')$  is given in (10).

Hence, the design criteria for minimizing the worst-case error is given by the optimization problem  $\min_C \mathcal{V}(C)$ .  $\mathcal{V}(C)$  corroborates the observations from Theorem III.1, and relates the worst-case error to the model only through the distances between channel outputs. In addition, we use the same tools as in Theorem III.2 to quantify the worst-error error decay with respect to system parameters. For an interpretation and a proof of the Theorem III.3 please refer to Sections III-C and V-C of [12].

### Theorem III.3 (Minimax Bound)

The worst-case error is bounded as:

$$\mathcal{M}(C) \geq \frac{32\pi^2 \lambda^2 \sigma^2 D^4}{27K^2 \|X^{\text{tag}}\|_F^2 \sum_{t=1}^T \|\tilde{B}_t\|_F^2 \|r(\mathbf{c}_t)\|^2} \quad (15)$$

where  $\tilde{B}_t = (I - BR_t)^{-1}$  and  $D$  is an approximate range between the tagged object and the antennas.

### C. Structure of the optimal codes

Finding the codes that minimize  $\mathcal{U}(C)$  and  $\mathcal{V}(C)$  is a combinatorial optimization problem. Performing an exhaustive search has a running time of  $\mathcal{O}(2^{NT})$  if wish to look for the best code of size  $T$ . Hence, finding the best code using brute-force is intractable except when the number of tags  $N$ , and the size of the code  $T$ , are very small.

Therefore, we introduce the idea of code proportions which is essential in reducing the search space. We show that our performance measures depend on the code only through the particular proportions of each codeword (see Theorem III.4). Let  $C = [\mathbf{c}_1 \cdots \mathbf{c}_T]$  be any code, then we define the proportion of code configuration  $\mathbf{c} \in \{0, 1\}^N$  in  $C$  as

$$\pi_{\mathbf{c}} = \frac{1}{T} \sum_{t=1}^T \mathbf{1}_{\mathbf{c}=\mathbf{c}_t}, \quad (16)$$

where  $\mathbf{1}_{\mathbf{c}=\mathbf{c}_t}$  is the indicator of the event  $\{\mathbf{c} = \mathbf{c}_t\}$ . In other words,  $\pi_{\mathbf{c}}$  is the relative proportion of occurrences of  $\mathbf{c}$  in  $T$ . Moreover, let  $\pi = [\pi_{\mathbf{c}^{(1)}}, \dots, \pi_{\mathbf{c}^{(M)}}]^T$  be the vector of code proportions, where  $\mathbf{c}^{(1)}, \dots, \mathbf{c}^{(M)}$  is an enumeration of all codewords. It is straightforward to see that if two coding matrices share the same size  $T$ , and the same proportions vector  $\pi$ , then they are permutations of one another. In what follows, instead of directly using the code  $C$ , we search for the optimal code through the proportions vector  $\pi$ .

The following theorem allows us to analyze the effect of  $C$  on the average and worst-case errors through the proportions vector  $\pi$ . Moreover, we show that the derived bounds in (13) and (14) can be written in terms of  $\pi$ . The proof of the following results are given in Section V-D of [12].

### Theorem III.4

Assuming independent and identically distributed noise,  $\mathcal{L}(C)$  and  $\mathcal{M}(C)$  only depend on the code  $C$  through  $\pi$ .

### Lemma III.1

If we fix  $T$ , the size of the code  $C$ , then we can write the minimization of  $\mathcal{U}(C)$  and  $\mathcal{V}(C)$  in term of  $\pi$  respectively as:

$$\mathcal{U}(\pi) = \sum_{Q, Q' \in \mathcal{Q}} \text{erfc} \left( \sqrt{\frac{T \langle \pi, \mathbf{g}(Q, Q') \rangle}{8\sigma^2}} \right) \theta(Q, Q'), \quad (17)$$

$$\mathcal{V}(\pi) = \max_{Q, Q' \in \mathcal{Q}} \exp \left( -\frac{T \langle \pi, \mathbf{g}(Q, Q') \rangle}{2\sigma^2} \right) \theta(Q, Q'), \quad (18)$$

where  $\mathbf{g}(Q, Q') \in \mathbb{R}^M$  is given by  $g(Q, Q')_i = \|f(Q; \mathbf{c}^{(i)}) - f(Q'; \mathbf{c}^{(i)})\|_2$ .

Theorem III.4 and Lemma III.1 allow us to write our design criteria as optimization problems with respect to the proportions vector  $\pi$ . In other words, the design criteria for the average and worst-case errors are equivalent to  $\min_{\pi} \mathcal{U}(\pi)$  and  $\min_{\pi} \mathcal{V}(\pi)$ , respectively.

## IV. NUMERICAL SIMULATIONS

### A. Simulation Setup

We use  $N = 4$  backscatter tags placed in a tetrahedron configuration 0.25m away from the center. Each tag can have two states, with reflection coefficients  $-0.5$  and  $0.5$ .  $K = 4$  full-duplex antennas are arranged in a  $1\text{m} \times 1\text{m}$  square on a plane 4m away from the center (see Figure 7 for a sample arrangement). Each antenna emits an identical signal  $s_k = 1$  for all  $k = 1, \dots, K$ . We use a wavelength  $\lambda = 0.005\text{m}$ , and a set of orientations  $\mathcal{Q}$  with  $|\mathcal{Q}| = 4000$ .

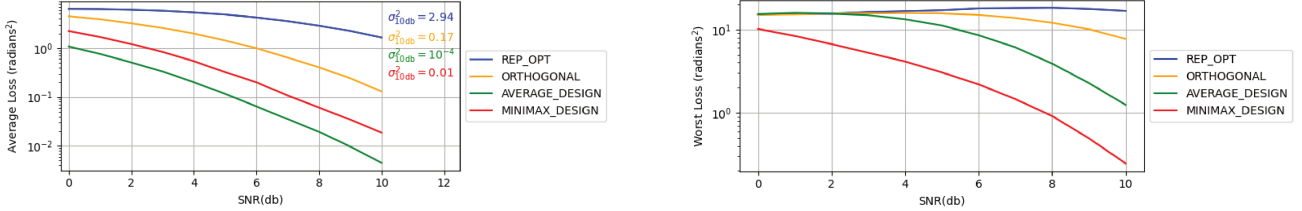


Fig. 5: The average (left) and worst-case (right) errors versus SNR for the tag array in Figure 7.

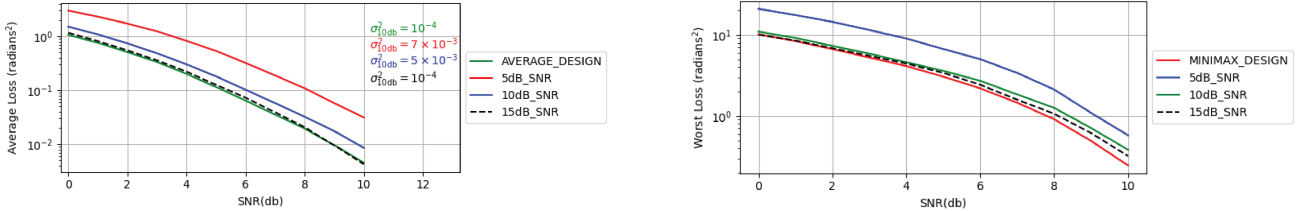


Fig. 6: The average (left) and worst-case error (right) of the designed codes for different levels of channel estimation errors.

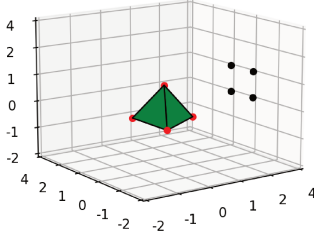


Fig. 7: An example of a simulation setup. The tags (given by the red dots) are in a tetrahedron configuration, while the antennas (given by the black dots) are in a square configuration.

We define SNR as *signal-to-noise ratio*, the received signal strength at each antenna, divided by the noise power. We test each value of  $\text{SNR} = 0, 1, \dots, 10 \text{ dB}$ , with 500 trials for each of the 4000 "ground truth" orientations in  $\mathcal{Q}$ . As a measure of distance, we use the polar and azimuthal angles in the polar coordinate system  $(r, \theta, \varphi)$ . The performance of a code varies across different orientations. Hence, unique to average error trials, we have included the variance of each coding method at an SNR value of 10dB. In the simulation trials, we use codes of size  $T = 24$ , and compare the performance of the following methods:

- REP\_OPT: The best repetition code (all  $T = 24$  code-words used are the same). This method is equivalent to the design criteria suggested in [9].
- ORTHOGONAL: The code where each of the vectors in the standard basis  $\{e_1, \dots, e_4\}$  is used 6 times.
- AVERAGE DESIGN: The method we suggested to minimize the average error; i.e., the coding scheme that minimizes  $\mathcal{U}(\pi)$ .
- MINIMAX DESIGN: The method we suggested to minimize the worst-case error; i.e., the coding scheme that minimizes  $\mathcal{V}(\pi)$ .

### B. The Average and Worst-Case Errors

The results shown in Figure 5 suggest that channel knowledge at the receiver provides significant benefits over orthogonal codes. For the tetrahedron tag configuration shown in Figure 7, the average error when using the code AVERAGE DESIGN is  $70\times$  lower than the error obtained when using orthogonal codes. Meanwhile, MINIMAX DESIGN offers an error that is  $100\times$  lower for the worst-case error. Furthermore, the performance obtained when using the best static code is consistently the worst out of the considered methods.

We tested the performance on our design criteria on random tag array configurations different than the one shown in Figure 7. In almost half of all trials, the designed codes offered more than a  $10\times$  improvement for the average error, and a  $20\times$  improvement for the worst-case error. Please refer to Sections IV-B and IV-C of [12] for more details.

### C. Robustness

Computing the coding schemes suggested by our design criteria requires channel knowledge. However, since it is unlikely to have perfect channel knowledge, we test the performance of our design criteria when computed using imperfect channel estimation. We introduce channel estimation errors by adding noise to the channel outputs in different orientations. Specifically, instead of using  $F(Q; C)$  to compute the suggested coding scheme, we use

$$F'(Q; C) = F(Q; C) + W_Q, \quad (19)$$

where  $W_Q$  is white Gaussian noise, and  $W_Q$  is independent of  $W_{Q'}$  for every  $Q' \neq Q$ . We tested the following values of the SNR = 5, 10, 15dB, with 50 trials each, and then averaged the performance. In particular, the results of Figure 6 indicate that our designed codes retain nearly all their improvements when computed with channel estimation errors greater than or equal to 10dB.

## REFERENCES

- [1] A. Saxena, J. Driemeyer, and A. Y. Ng, "Learning 3-d object orientation from images," in *2009 IEEE International Conference on Robotics and Automation*, 2009, pp. 794–800.
- [2] A. Collet, D. Berenson, S. S. Srinivasa, and D. Ferguson, "Object recognition and full pose registration from a single image for robotic manipulation," in *2009 IEEE International Conference on Robotics and Automation*, 2009, pp. 48–55.
- [3] H. Fujiyoshi, T. Nagahashi, and S. Shimizu, *Robust and Accurate Detection of Object Orientation and ID without Color Segmentation*, 12 2007.
- [4] T. Starner, B. Leibe, D. Minnen, T. Westyn, A. Hurst, and J. Weeks, "The perceptive workbench: Computer-vision-based gesture tracking, object tracking, and 3d reconstruction for augmented desks," *Machine Vision and Applications*, vol. 14, pp. 59–71, 01 2003.
- [5] E. Soltanaghaei, A. Prabhakara, A. Balanuta, M. Anderson, J. M. Rabaey, S. Kumar, and A. Rowe, "Millimetro: Mmwave retro-reflective tags for accurate, long range localization," in *Proceedings of the 27th Annual International Conference on Mobile Computing and Networking*, ser. MobiCom '21. New York, NY, USA: Association for Computing Machinery, 2021, p. 69–82. [Online]. Available: <https://doi.org/10.1145/3447993.3448627>
- [6] E. Soltanaghaei, A. Dongare, A. Prabhakara, S. Kumar, A. Rowe, and K. Whitehouse, "Tagfi: Locating ultra-low power wifi tags using unmodified wifi infrastructure," *Proc. ACM Interact. Mob. Wearable Ubiquitous Technol.*, vol. 5, no. 1, Mar. 2021. [Online]. Available: <https://doi.org/10.1145/3448082>
- [7] T. Wei and X. Zhang, "Gyro in the air: tracking 3d orientation of battery-less internet-of-things," in *Proceedings of the 22nd Annual International Conference on Mobile Computing and Networking*. ACM, 2016, pp. 55–68.
- [8] A. A. N. Shirehjini, A. Yassine, and S. Shirmohammadi, "An rfid-based position and orientation measurement system for mobile objects in intelligent environments," *IEEE Transactions on Instrumentation and Measurement*, vol. 61, no. 6, pp. 1664–1675, 2012.
- [9] K. Chang, N. Raymondi, A. Sabharwal, and S. N. Diggavi, "Wireless paint: Code design for 3D orientation estimation with backscatter arrays," in *IEEE International Symposium on Information Theory, ISIT*. IEEE, 2020, pp. 1224–1229.
- [10] C. Jiang, Y. He, X. Zheng, and Y. Liu, "Orientation-aware rfid tracking with centimeter-level accuracy," in *Proceedings of the 17th ACM/IEEE International Conference on Information Processing in Sensor Networks*. IEEE Press, 2018, pp. 290–301.
- [11] X. Fu, A. Pedross-Engel, D. Arnitz, and M. S. Reynolds, "Simultaneous sensor localization via synthetic aperture radar (sar) imaging," in *2016 IEEE SENSORS*, Oct 2016, pp. 1–3.
- [12] M. R. Rammal, S. Diggavi, and A. Sabharwal, "Coded estimation: Design of backscatter array codes for 3d orientation estimation," 2021. [Online]. Available: <https://arxiv.org/abs/2112.00883>
- [13] D. Tse and P. Viswanath, *Fundamentals of Wireless Communication*. USA: Cambridge University Press, 2005.
- [14] A. Sabharwal, P. Schniter, D. Guo, D. W. Bliss, S. Rangarajan, and R. Wichman, "In-band full-duplex wireless: Challenges and opportunities," *IEEE Journal on selected areas in communications*, vol. 32, no. 9, pp. 1637–1652, 2014.
- [15] A. N. Shirayev and Y. A. Koshevnik, "Review: Lucien le cam, asymptotic methods in statistical decision theory," *Bull. Amer. Math. Soc. (N.S.)*, vol. 20, no. 2, pp. 280–285, 04 1989. [Online]. Available: <https://projecteuclid.org:443/euclid.bams/1183555039>